PHENOMENOLOGY OF THE STRONG INTERACTION AT HIGH ENERGIES

WE REVIEW BRIEFLY A NUMBER OF FEATURES OF THE STRONG INTERACTION AT HIGH ENERGIES. BY 'HIGH' WE MEAN $E_{CM} \gtrsim 2$ GeV WHERE RESONANCE PRODUCTION EFFECTS NO LONGER ARE THE DOMINANT FEATURE IN SCATTERING PROCESSES. THE DATA COLLECTED AT THESE HIGH ENERGIES HAVE LARGELY DEFIED ANY FUNDAMENTAL INTERPRETATION (IN DETAIL). BUT A CULTURAL APPRECIATION OF HIGH ENERGY PHYSICS REQUIRES SOME EXPOSURE TO THE PHENOMENA DISCUSSED IN THIS LECTURE.

1. TOTAL CROSS SECTIONS

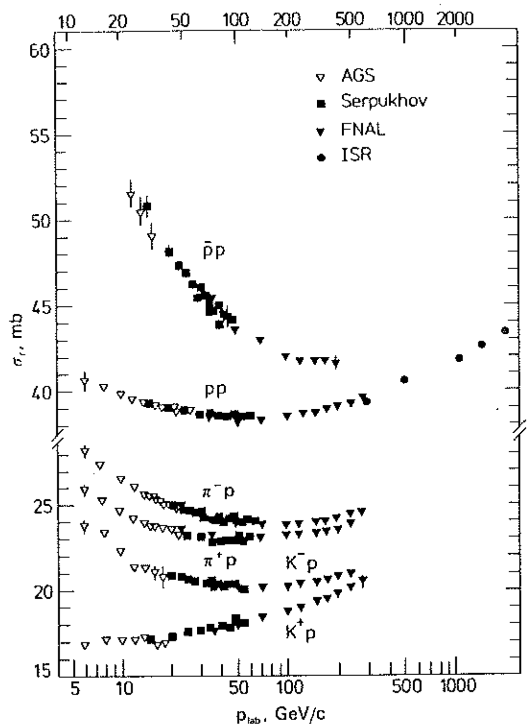

Fig. 4.30 Total cross-sections for various particles on proton targets.

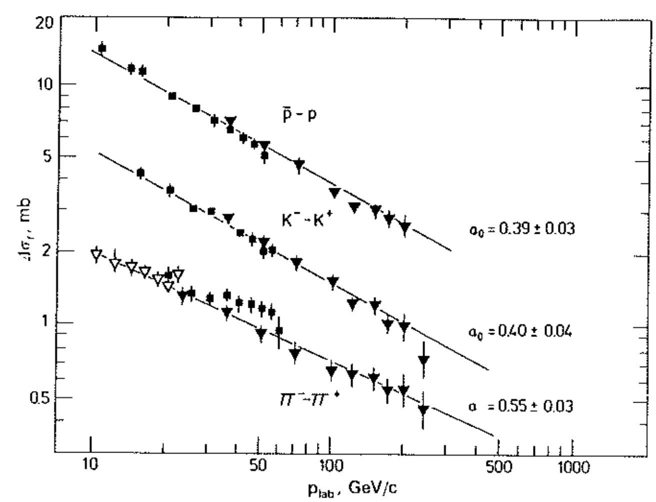

Fig. 4.31 Difference of antiparticle and particle cross-sections on protons as a function of energy.

THE ENERGY DEPENDENCE OF THE TOTAL CROSS SECTIONS IS NOT WELL UNDERSTOOD. PRIOR TO 1972 DATA WERE AVAILABLE ONLY UP TO $P_{LAB} = 70$ GeV/c BELOW WHICH MOST CROSS SECTIONS WERE FALLING WITH ENERGY. AS SUCH MOST 'PREDICTIONS' OF THAT ERA WERE THAT THE TOTAL CROSS SECTIONS WOULD APPROACH A CONSTANT AT VERY HIGH ENERGIES.

ONE SYSTEMATIC TREND OF NOTE IS THAT $\sigma_{ap} - \sigma_{\bar{a}p} \to 0$ AS ENERGY INCREASES. THERE IS AN 'EXPLANATION' FOR THIS, THE SO-CALLED 'POMERANCHUK THEOREM', SOV. PHYS. JETP 7, 499 (1958), BUT THIS IS ONE OF THE LESS FUNDAMENTAL RESULTS OF FIELD THEORY.

AS REMARKED IN LECTURE 2, $\sigma_{pp} \sim 40$ mb $\Rightarrow$ 'RADIUS' OF PROTON ~ 1.2 FERMIS, SOMEWHAT LARGER THAN INFERRED FROM ep ELASTIC SCATTERING, LECTURES 6 & 7. WE REMIND YOU THAT $\sigma_{\pi p}/\sigma_{pp} \sim 2/3$, CONSISTENT WITH A SIMPLE QUARK MODEL.

2. Elastic Cross Sections

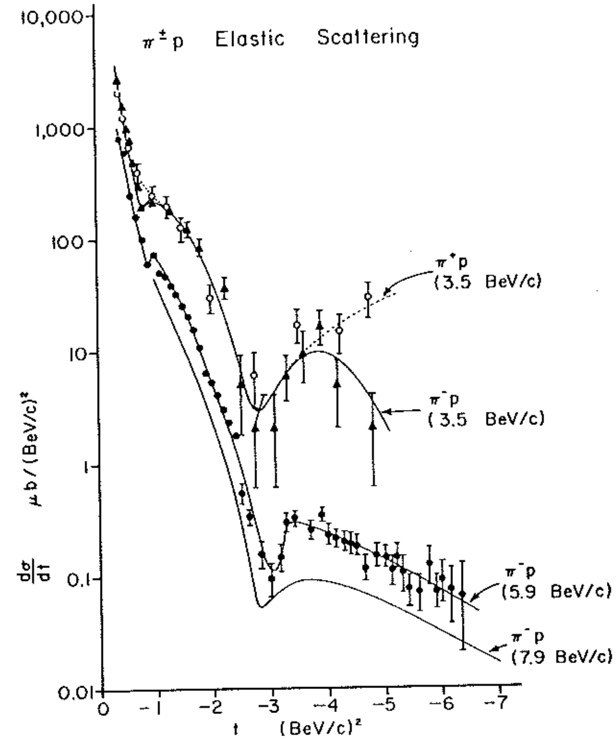

Structure in $\pi^{\pm}p$ elastic scattering data at large momentum transfers.

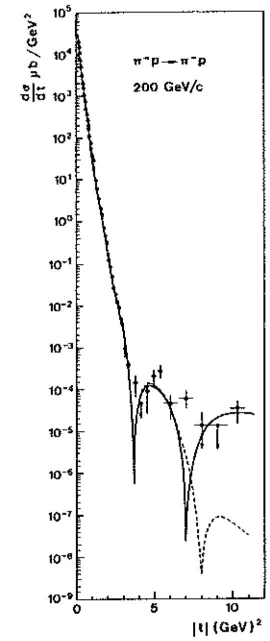

Fig. 1. π^-p elastic scattering data at 200 GeV/c (ref. [4] and ref. [15]). Solid curve from parametrization (3). Dashed curve from ref. [10].

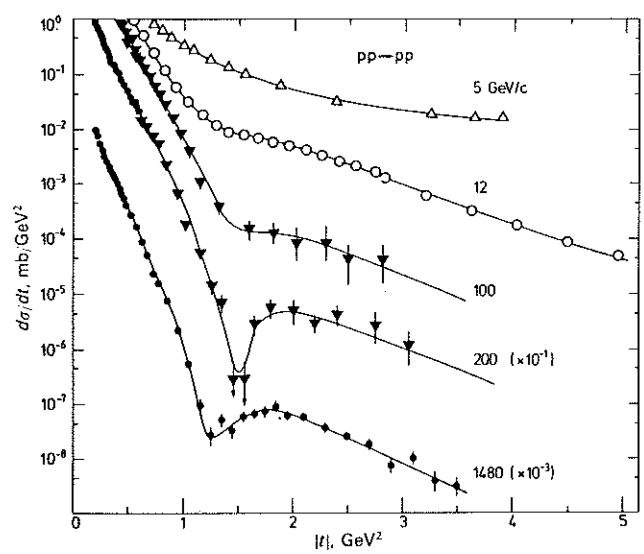

Fig. 4.33 Differential cross-section for elastic *pp* scattering as a function of the square of the momentum transfer, $|t| = q^2$.

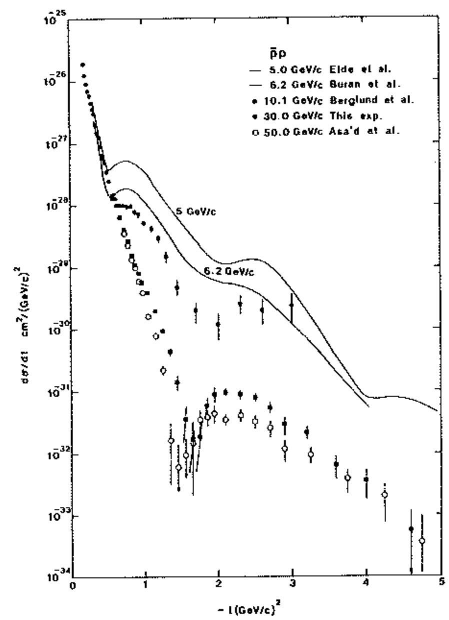

Fig. 3. $\bar{p}p$ elastic differential cross section at 30 GeV/c (this experiment), compared with $\bar{p}p$ data at 5.0 [9], 6.2 [10], 10.1 [11] and 50 [2] GeV/c. The data from refs. [9] and [10] are presented as smoothed curves.

The elastic cross section results have been given a semi-classical interpretation in terms of an optical model. In Ph 206, Lecture 17, we show that the classical cross section for the scattering of light of wave number k (= momentum if $\hbar = 1$) by a totally absorbing disk of radius R is

$$\frac{d\sigma}{d\Omega} = k^2 R^4 \left| \frac{J_1(kR\sin\theta)}{kR\sin\theta} \right|^2$$

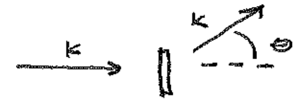

To compare with the present cases note that $t = q^2 = -k^2 \sin^2 \theta/2$

so $\dfrac{d\sigma}{dt} = \dfrac{d\sigma}{dq^2} \propto \pi R^4 \left| \dfrac{J_1(qR)}{qR} \right|^2$

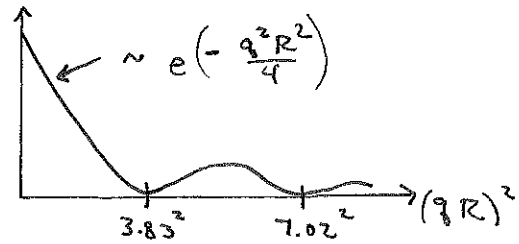

At small q^2 this falls off exponentially, but vanishes when $qR = 3.83, 7.02 \ldots$

or when $q^2 = \dfrac{.57}{R^2}, \dfrac{1.91}{R^2} \ldots$ for R measured in fermis, q^2 in GeV^2

From the lower energy scattering data we might infer

- $R \sim .8$ f from πp scattering
- $R \sim 1$ f from $\bar{p}p$
- $R \sim .6$ f from pp

However, the positions and depths of the 'diffraction minima' appear to change with energy. Typically the shifts in position of the dips can be correlated with changes in R inferred from the total cross section measurements. Note that a 'black disk' model would also predict $\sigma_t \approx 2\,\sigma_{elastic}$, as noted on p. 206. But the data (p25) show $\sigma_t \sim 5\,\sigma_{el}$. One is left with a rather crude picture of a hadron as a partially opaque disk whose radius varies with the interaction energy.

A variation on the optical model tries to incorporate the form factor information obtained from ep elastic scattering [Wu & Yang, P.R. 137, 3708 (1965)]. They supposed that the pp scattering might be due to a diagram like

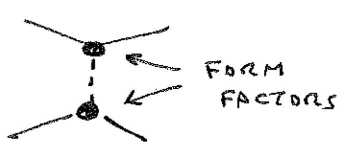

Each vertex is proportional to the form factor $G_E(q^2)$ obtained on p. 100. The thought is that the electric charge distribution might also be the relevant matter distribution for the strong interaction in case of elastic scattering. Then

$$\sigma_{pp} \propto \left[G_E(q^2)\right]^4$$

There is some truth to this, but...

See Chou & Yang, Phys. Lett, 128B, 457 (1983) for recent comments.

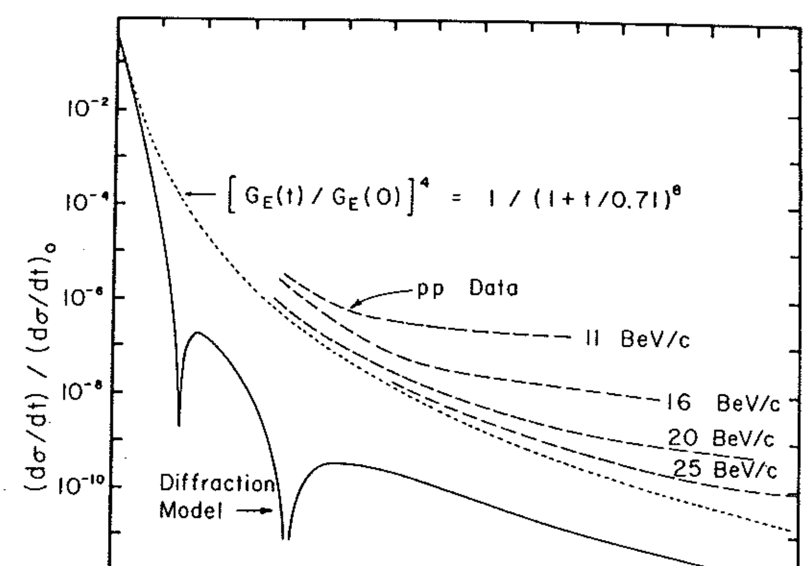

Figure 5.12. Predictions of the hadron density model for *pp* elastic scattering are shown by the solid curve. Experimental values of $(d\sigma/dt)/(d\sigma/dt)_{t=0}$ are represented by the dashed curves. The dotted curve denoted the dipole approximation to the proton electromagnetic structure data: from L. Durand, III and R. Lipes, *Phys. Rev. Letters* 20, 637 (1968).

3. FORWARD AND BACKWARD PEAKS IN 2 BODY SCATTERING

[REFERENCE FOR SECS 3 & 4: 'PHENOMENOLOGICAL THEORIES OF HIGH ENERGY SCATTERING' BY BARGER & CLINE, BENJAMIN, 1969.]

WE HAVE MENTIONED HOW THE PARTIAL WAVE ANALYSIS IS ESPECIALLY SUITABLE FOR SCATTERING IN WHICH AN INTERMEDIATE RESONANT STATE IS FORMED. FOR C.M. ENERGIES ABOVE A FEW GeV THERE IS NO LONGER MUCH EVIDENCE OF SUCH RESONANCES IN PARTICLE SCATTERING. RATHER, THE COMMON SITUATION IN A SIMPLE REACTION $a+b \to c+d$ IS THAT THE INTERACTION TAKES PLACE VIA PARTICLE EXCHANGE.

IT IS USEFUL TO RECALL THE 'MANDELSTAM VARIABLES' INTRODUCED IN LECTURE 3, p32.

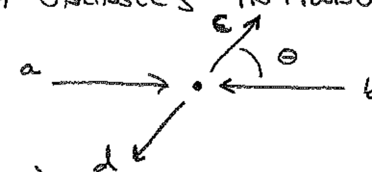

VIEW IN C.M. FRAME

$$s = (a+b)^2 = (c+d)^2 = E_{CM}^2$$

$$t = (a-c)^2 = (d-b)^2 = m_a^2 + m_c^2 + 2(E_a E_c - P_a P_c \cos\theta)$$

$$u = (a-d)^2 = (c-b)^2 = m_a^2 + m^2 + 2(E_a E_d + P_a P_d \cos\theta)$$

$$s + t + u = m_a^2 + m_b^2 + m_c^2 + m_d^2$$

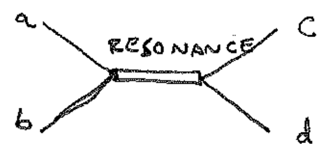

SCATTERING VIA RESONANCE PRODUCTION IS SAID TO BE AN S-CHANNEL PROCESS IN THAT

$s = M_R^2$ AND PROPAGATOR $\sim \dfrac{1}{s - M_R^2 + i M_R \Gamma_t}$ $\Rightarrow \sigma \sim \dfrac{\Gamma_{ab}\Gamma_{cd}}{(s-M_R^2)^2 + M_R^2 \Gamma_t^2}$

CORRECTION TO PROPAGATOR FOR FINITE LIFETIME

RELATIVISTIC BREIT-WIGNER RESONANCE FORMULA

IF THE SCATTERING TAKES PLACE VIA PARTICLE EXCHANGE, THERE ARE 2 TYPES OF DIAGRAMS:

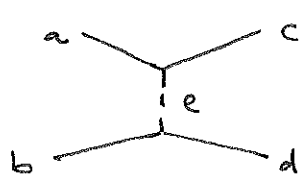

t-CHANNEL EXCHANGE

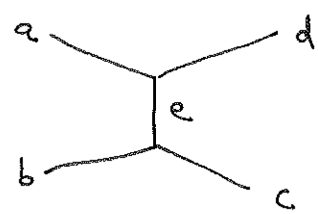

u-CHANNEL EXCHANGE

$t = $ (VIRTUAL MASS OF EXCHANGED PARTICLE)^2 $\qquad$ $u = $ (VIRTUAL MASS OF EXCHANGED PARTICLE)^2

M_e = REST MASS OF EXCHANGED PARTICLE

PROPAGATOR $\sim \dfrac{1}{t - M_e^2}$ $\qquad$ PROPAGATOR $\sim \dfrac{1}{u - M_e^2}$

$\sigma \sim \dfrac{1}{(1-\cos\theta)^2}$ $\qquad$ $\sigma \sim \dfrac{1}{(1+\cos\theta)^2}$

$\Rightarrow$ FORWARD PEAK $\qquad$ $\Rightarrow$ BACKWARD PEAK

Ph 529 Lecture 12

IN A SIMPLE REACTION LIKE $\pi^- p$ ELASTIC SCATTERING THE t-CHANNEL REACTION MIGHT BE DUE TO ρ EXCHANGE

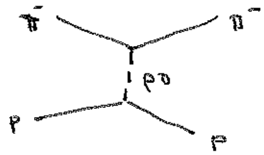

[π EXCHANGE IS FORBIDDEN BY G-PARITY]

THE u-CHANNEL REACTION MIGHT BE DUE TO Δ EXCHANGE

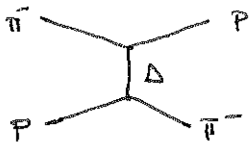

[NUCLEON EXCHANGE IS FORBIDDEN, BECAUSE IN THE u-CHANNEL WE HAVE $\ell \to \pi^- \bar{p}$ WHICH HAS $I_3 = -3/2$.]

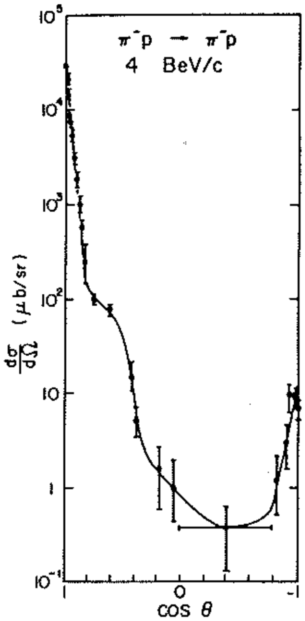

Figure 2.6. Forward and backward peaks in $\pi^- p$ elastic scattering at 4 BeV/c.

IN MESON-BARYON SCATTERING THE t-CHANNEL REACTION IS ALWAYS DUE TO MESON EXCHANGE, WHILE THE u-CHANNEL REACTION IS DUE TO BARYON EXCHANGE.

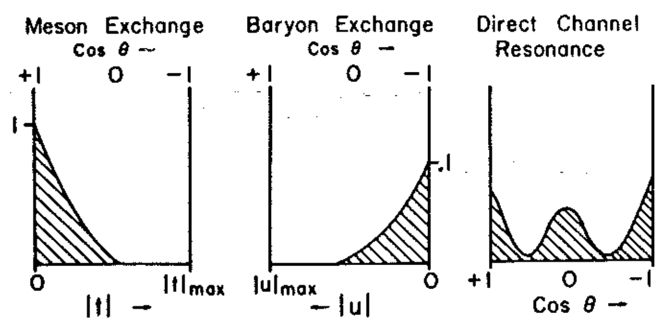

Figure 2.2. Pictorial illustration of meson exchange, baryon exchange, and direct channel resonances. Qualitative predictions for scattering via these mechanisms are illustrated.

THE TABLE PRESENTS A CATALOG OF FORWARD AND BACKWARD PEAKS OBSERVED IN VARIOUS REACTIONS. THE PRESENCE OR ABSENCE OF THESE PEAKS CORRELATES WELL WITH THE EXISTENCE OF MESONS OR BARYONS WITH THE PROPER QUANTUM NUMBERS TO BE EXCHANGED.

REACTION	t-CHANNEL QUANTUM NUMBERS Q_t	I_t	Y_t	MESONS WITH THESE QUANTUM NUMBERS	FORWARD PEAK?	u-CHANNEL QUANTUM NUMBERS Q_u	I_u	Y_u	BARYONS WITH THESE QUANTUM NUMBERS	BACKWARD PEAK?
$\pi^+ p \to \{\pi^+, \rho^+\} p$	0	0,1	0	YES, ρ	YES	0	$\frac{1}{2},\frac{3}{2}$	1	n YES Δ^0	YES
$\pi^- p \to \{\pi^-, \rho^-\} p$	0	0,1	0	YES ρ	YES	2	$\frac{3}{2}$	1	YES Δ^{++}	YES
$\pi^- p \to \{\pi^0, \rho^0\} n$	1	1	0	YES ρ	YES	1	$\frac{1}{2},\frac{3}{2}$	1	p YES Δ^+	YES
$K^+ p \to \{K^+, K^{*+}\} p$	0	0,1	0	π, YES, ρ	YES	0	0,1	0	Λ YES Σ^0	YES
$K^- p \to \{K^-, K^{*-}\} p$	0	0,1	0	π YES ρ	YES	2	1	2	NO	NO
$K^+ n \to \{K^0, K^{*0}\} p$	-1	1	0	π YES ρ	YES	0	0,1	0	Λ YES Σ^0	YES
$K^- p \to \{\bar{K}^0, \bar{K}^{*0}\} n$	1	1	0	π YES ρ	YES	1	0,1	2	NO	NO
$\pi^- p \to K^0 \Lambda$	1	$\frac{1}{2}$	1	YES K	YES	1	1	0	YES Σ^+	YES
$\pi^- p \to K^+ \Sigma^-$	2	$\frac{3}{2}$	1	NO	NO	0	0,1	0	Λ YES Σ^0	YES
$\pi^+ p \to K^+ \Sigma^+$	0	$\frac{1}{2},\frac{3}{2}$	1	YES K	YES	0	0,1	0	Λ YES Σ^0	YES
$K^- p \to K^+ \Xi^-$	2	1	2	NO	NO	0	0,1	0	Λ YES Σ^0	YES
$K^- p \to K^0 \Xi^0$	1	0,1	2	NO	NO	1	1	0	YES Σ^+	YES
$K^- p \to (K^+ K^0) \Omega^-$	2	$\frac{1}{2}$	3	NOT KNOWN	?	0	$\frac{1}{2}$	-1	YES Ξ^-	?
$\pi^- p \to \pi^+ N^{*-}$	2	2	0	NO	NO	0	$\frac{1}{2},\frac{3}{2}$	1	n YES Δ^0	YES
$\pi^+ p \to \pi^0 N^{*++}$	-1	1,2	0	YES ρ	YES	1	$\frac{1}{2},\frac{3}{2}$	1	p YES Δ^+	YES
$K^- p \to \{\pi^+, \rho^+\} \Sigma^-$	2	$\frac{3}{2}$	1	NO	NO	0	$\frac{1}{2},\frac{3}{2}$	1	n YES Δ^0	YES
$K^- p \to \{\pi^-, \rho^-\} \Sigma^+$	0	$\frac{1}{2},\frac{3}{2}$	1	YES K	YES	2	$\frac{3}{2}$	1	YES Δ^{++}	YES
$\bar{p} p \to \bar{\Lambda} \Lambda$	1	$\frac{1}{2}$	+1	YES K	YES	1	$\frac{1}{2}$	1	B=2	NO
$\bar{p} p \to \bar{\Lambda} \Sigma^0$ or $\bar{\Sigma}^0 \Lambda$	1	$\frac{1}{2}$	+1	YES K	YES	1	$\frac{1}{2}$	1	B=2	NO
$\bar{p} p \to \bar{\Sigma}^- \Sigma^-$	2	$\frac{3}{2}$	+1	NO	NO	0	$\frac{1}{2},\frac{3}{2}$	1	B=2	NO
$\bar{p} p \to \bar{\Sigma}^+ \Sigma^+$	0	$\frac{1}{2},\frac{3}{2}$	+1	YES K	YES	2	$\frac{3}{2}$	1	B=2	NO

Examples of reactions which are predicted to have forward or backward peaks, but not both (except the 1st).

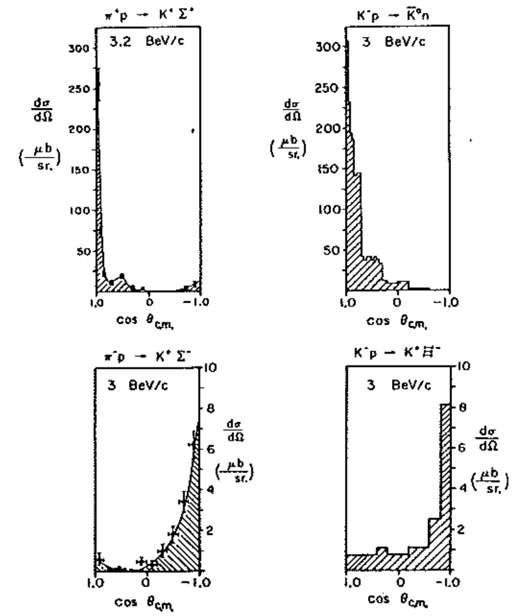

Figure 2.8. Differential cross section data at 3 BeV/c for the inelastic reactions $\pi^+p \to K^+\Sigma^+$, $K^-p \to \bar{K}^0 n$, $\pi^-p \to \Sigma^-K^+$, and $K^-p \to K^+\Xi^-$: from V. Barger, *Rev. Mod. Phys.* 40, 129 (1968).

4. Reggeology

As more and more particles (resonances) were discovered, it was noted [Regge, Nuovo Cimento 14, 951 (1959), Chew & Frautschi, P.R.L. 7, 394 (1961)] that they could be organised into interesting patterns if one plots spin vs. mass squared.

$M^2 \equiv u$ for baryons

$M^2 \equiv t$ for mesons

$$\boxed{\tau \equiv \begin{cases} (-1)^{J-\frac{1}{2}} & \text{for baryons} \\ (-1)^{J} & \text{for mesons} \end{cases}}$$

is called the signature

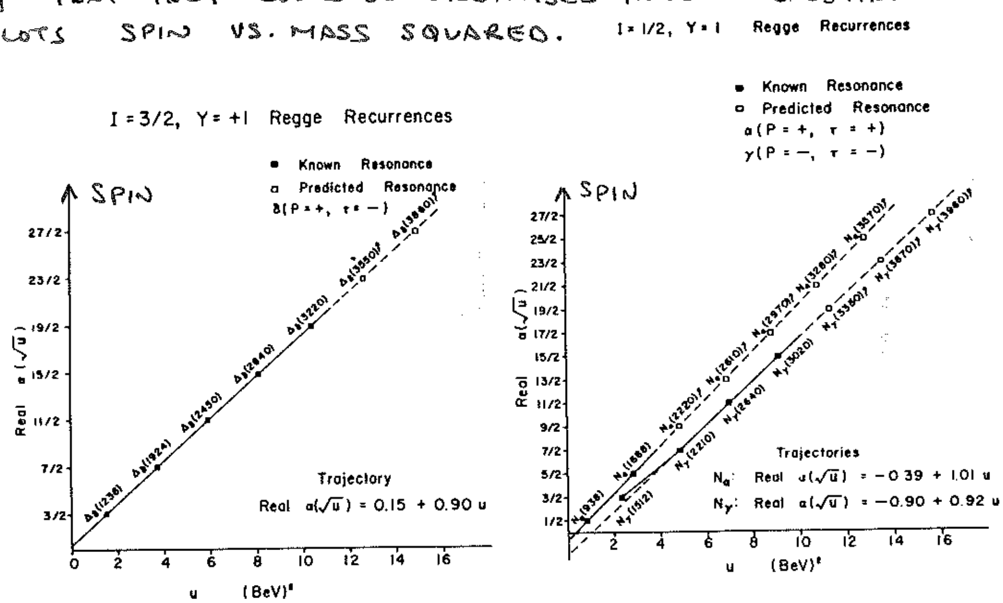

Figure 1.4. Particle recurrences on Δ_δ, N_α, and N_γ baryon Regge trajectories: from V. Barger and D. Cline, *Phys. Rev. Letters* 16, 913 (1968).

Essentially all known particles can be placed on a family of lines, or Regge trajectories of nearly unit slope (if m^2 is measured in GeV^2). The particles are spaced in steps of $\Delta J = 2$, so that each trajectory has either odd or even parity.

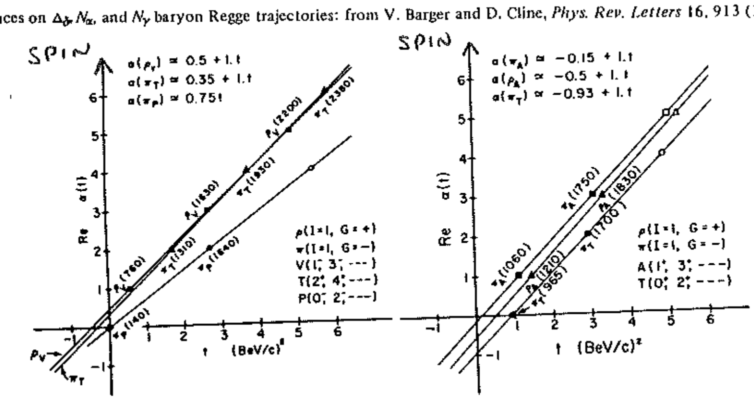

Figure 1.5. Tentative assignments of $I = 1$ mesons to Regge trajectories.

WHEN THIS CLASSIFICATION WAS FIRST NOTED IT WAS HOPED THAT IT WOULD PROVIDE FUNDAMENTAL NEW INSIGHT INTO THE NATURE OF ELEMENTARY PARTICLES. SO FAR THIS HAS NOT BEEN THE CASE. INSTEAD THE SU(3) CLASSIFICATION AND THE QUARK MODEL HAVE PROVED MORE FRUITFUL.

AFTER THE ψ FAMILY OF $c\bar{c}$ QUARK STATES WAS DISCOVERED IT WAS REALIZED THAT MANY FEATURES OF QUARK BOUND STATES ARE REPRODUCED IN A NON-RELATIVISTIC MODEL WITH A LINEAR POTENTIAL FOR THE COLOR FORCE FIELD. CRUDELY, THE MYSTERIOUS PROPERTY OF COLOR CONFINEMENT RESTRICTS THE LINES OF COLOR FORCE INTO TUBES OR 'STRINGS' CONNECTING THE QUARKS.

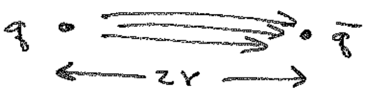

IF WE SUPPOSE MOST OF THE MASS OF THE $q\bar{q}$ STATE IS ACTUALLY IN THE ENERGY DENSITY OF THE COLOR FIELD, THEN

$$M = U \sim 2Kr$$

WITH $M \sim 1\,\text{GeV}$, $r \sim 1\,\text{FERMI}$, WE ESTIMATE $K \sim .1\,\text{GeV}^2$

IF THE $q\bar{q}$ SYSTEM IS ROTATING ABOUT AN AXIS $\perp$ TO THE STRING

THEN ANGULAR MOMENTUM $J = I\omega = \frac{1}{3}Mr^2\omega$, FOR A STRING OF LENGTH $2r$. THE CHARACTERISTIC VELOCITY OF THIS ROTATION IS $v = 1$ ($= c$) AS SEEN IN A FURTHER APPROXIMATION. SUPPOSE HALF THE MASS WERE AT EACH END OF THE STRING $\frac{M}{2} \bullet \xleftrightarrow{2r} \bullet M/2$

THEN $F = \nabla U = K = \frac{M}{2}\frac{v^2}{r} = Kv^2 \Rightarrow v = 1$

IF SO, $\omega = 1/r$ AND $\underline{J} = \frac{1}{3}Mr = \frac{M^2}{6K} \approx \underline{1.7\,M^2}$

USING $K \sim .1\,\text{GeV}^2$. MAYBE.

WE RETURN TO THE REGGE TRAJECTORIES. PREVIOUSLY (SEC 3) WE HAD A PICTURE OF PARTICLE SCATTERING VIA ONE PARTICLE EXCHANGE, BUT NOW WE COULD EXCHANGE ANY MEMBER OF A POSSIBLY INFINITE FAMILY. WE SAY THAT THE ENTIRE REGGE TRAJECTORY IS EXCHANGED.

WITHOUT PROOF WE CLAIM THAT THE AMPLITUDE FOR EXCHANGE OF A SPIN J PARTICLE GOES LIKE

$$\frac{-(s/s_0)^J}{t - M_J^2}$$

WHERE M_J = MASS OF THE PARTICLE OF SPIN J

s_0 = SOME ENERGY SCALE <u>NOT</u> SPECIFIED BY THE REGGE MODEL.

IT WAS THE s^J BEHAVIOR WHICH BOTHERED REGGE – IT LEADS TO CROSS SECTIONS WHICH RISE RAPIDLY WITH C.M ENERGY, IF HIGH SPIN EXCHANGE IS INVOLVED.

Then the amplitude for exchanging the entire Regge trajectory is

$$\sum_{\substack{J \text{ in} \\ \text{steps of } 2}} \frac{-(s/s_0)^J}{t - M_J^2} = b \sum_{\text{all } J} \frac{(-1)^J - 1}{a + bt - J} \left(\frac{s}{s_0}\right)^J \qquad \text{using } J = a + b M_J^2$$

The series can be summed:

$$\text{AMPL} \sim \frac{\pi b}{2} \frac{1 - e^{-i\pi\alpha}}{\sin \pi\alpha} \left(\frac{s}{s_0}\right)^{\alpha} \qquad \text{with } \alpha(t) = a + bt$$

This relation was originally derived by Regge via a transformation of the partial wave expansion in the complex angular momentum plane, rather than as a sum over Feynman diagrams.

The reaction cross section goes like (p 84)

$$\sigma \sim \frac{1}{s} |\text{AMPL}|^2 \sim (s/s_0)^{2a-1}$$

and the differential cross section is $\frac{d\sigma}{dt} \sim F(t) \left(\frac{s}{s_0}\right)^{2\alpha(t) - 2}$

$F(t)$ is slowly varying

Noting that $\alpha(t) = a + bt$, we can also write

$$\frac{d\sigma}{dt} \sim F(t) \left(\frac{s}{s_0}\right)^{2a-2} (s/s_0)^{2bt} \sim e^{2b \log s/s_0 \, t} \sim e^{-c|t|} \qquad (c>0)$$

Thus the differential cross section should fall exponentially with t, with a slope factor that increases with $(\log s)^2$. This implies that the forward peak appears to 'shrink' with increasing energy.

b in this figure is what we called c above.

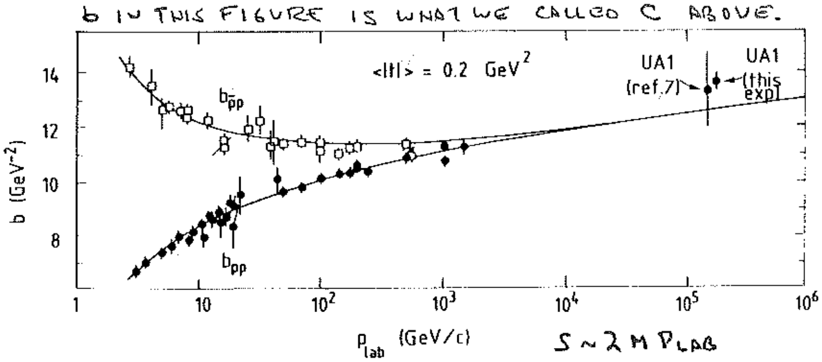

$s \sim 2 M P_{LAB}$

The logarithmic rise of the $\bar{p}p$ elastic cross section has been observed only recently. [Arnison et al. Phys Lett (1983)]

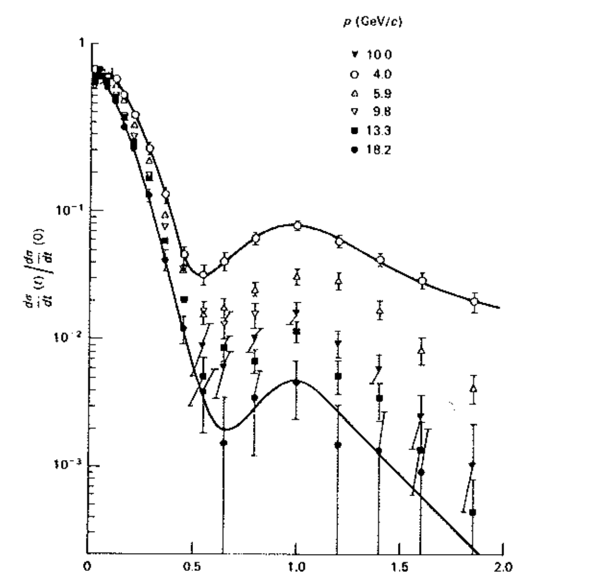

Fig. 4.41 Early observations on the differential cross-section for elastic charge exchange, $\pi^- p \to \pi^0 n$, compiled by Sonderegger *et al.* (1966). The shrinkage of the t-distribution with increasing incident momentum p yields $\alpha_\rho(t) = 0.6 + 0.9t$ for the ρ-exchange trajectory.

Ph 529 LECTURE 12

STRUCTURE AT LARGE t IS SAID TO BE DUE TO INTERFERENCE BETWEEN REGGE TRAJECTORIES, AS GENERALLY MORE THAN 1 CAN BE EXCHANGED. THIS IS QUITE COMPLICATED, AND OFFERS A RATHER DIFFERENT VIEW OF 'DIPS' IN THE CROSS SECTION FROM THAT OF THE OPTICAL MODEL.

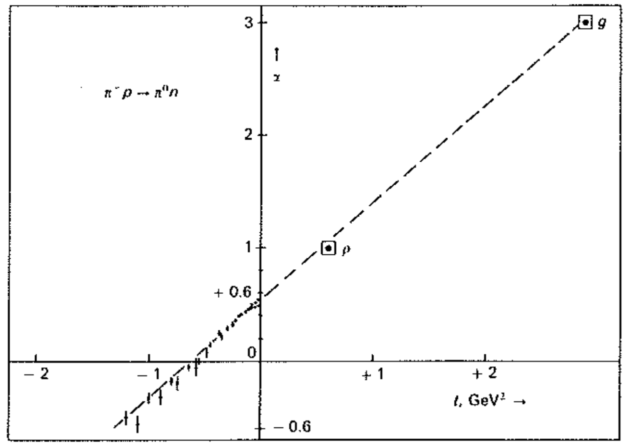

Fig. 4.42 The ρ-trajectory. For $t < 0$, the data come from the analysis of $\pi^- p$ charge-exchange scattering. The line drawn through it extrapolates fairly well through the resonances or poles of the ρ- and g-mesons in the region $t > 0$.

WE REMARK ON OUR RELATION $\sigma \sim (s/s_0)^{2a-1}$. EXPERIMENTALLY ELASTIC CROSS SECTIONS ARE ROUGHLY CONSTANT WITH ENERGY, WHICH WOULD REQUIRE $a \approx 1$. HOWEVER, KNOWN PARTICLE TRAJECTORIES ALL HAVE INTERCEPTS $\leq 1/2$, ACHIEVED FOR THE ρ AND ω TRAJECTORIES. TO SAVE THE REGGE MODEL THE 'POMERON' OR VACUUM TRAJECTORY WAS INVENTED. (NOWADAYS THIS WOULD BE CALLED GLUON EXCHANGE). THE TRAJECTORY PARAMETERS ARE $\alpha(t) \sim 1 + t$ (THE GLUON IS MASSLESS AND HAS SPIN 1; ARE THERE SPIN 3 'GLUEBALL' STATES???) THIS ALSO 'EXPLAINS' THE POMERANCHUK THEOREM, SINCE THE SAME POMERON TRAJECTORY CAN BE EXCHANGED IN BOTH $a p$ AND $\bar{a} p$ ELASTIC SCATTERING.

THE ENERGY DEPENDENCE OF OTHER REACTIONS IS NOW READILY PREDICTED. $\sigma \sim s^{2a-1} \sim P_{LAB}{}^{2a-1}$ WHERE a = INTERCEPT OF THE HIGHEST RELEVANT TRAJECTORY.

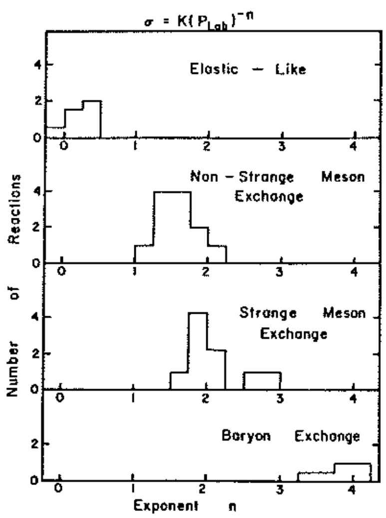

Figure 2.23. Momentum dependence $(p_{Lab})^{-n}$ for integrated cross sections: from D. Morrison, CERN Report 66-20.

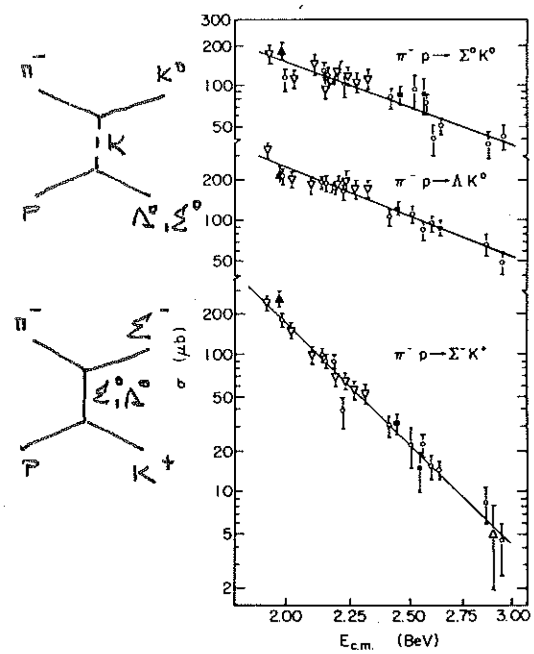

Figure 2.25. Energy dependence of integrated cross sections for $\pi^- p \to \Lambda K$, ΣK reactions: from O. Dahl *et al.*, *Phys. Rev.* **163**, 1430 (1967).

5. MULTIPARTICLE PRODUCTION

THE CROSS SECTIONS FOR 2 BODY SCATTERING, OTHER THAN ELASTIC SCATTERING FALL WITH ENERGY, BUT THE TOTAL CROSS SECTIONS PP, $\bar{\pi}$ P... ARE NEARLY CONSTANT. THIS CAN OCCUR BECAUSE AT HIGH ENERGY, MULTIPARTICLE PRODUCTION IS POSSIBLE. WHILE ANY PARTICULAR REACTION CROSS SECTION IS SMALL AND FALLING WITH ENERGY, THE NUMBER OF POSSIBLE REACTIONS INCREASES WITH ENERGY. IN THIS SECTION WE GIVE SOME OVERALL CHARACTERIZATIONS OF THE MULTIPARTICLE PRODUCTION PHENOMENA.

A PROMINENT FEATURE IS SIMPLY THE TOTAL NUMBER OF PARTICLES PRODUCED. WE DISCUSSED THIS BRIEFLY ON P. 57. THE AVERAGE NUMBER OF PARTICLES PRODUCED VARIES LIKE

$$\langle n \rangle \sim a + b \ln P_{LAB} \sim a + c \ln s$$

THE HIGHEST ENERGY REACTIONS STUDIED IN THE LABORATORY ARE $\bar{p}p$ COLLISIONS AT $\sqrt{s} = 540$ GeV, FOR WHICH $\langle n \rangle \approx 25$ CHARGED PARTICLES. AS REMARKED EARLIER THESE PARTICLES ARE MOSTLY PIONS, WITH ABOUT 10% KAONS AND 3% ANTIPROTONS (IF P BEAM). NOTE THAT $\langle n_p \rangle \sim 1.5$ IN THE FIGURE, FROM WHICH WE INFER THAT NEUTRON PRODUCTION IS ABOUT THAT OF K^+. OTHER NEUTRAL PARTICLES INCLUDE π^0 ($\to 2\gamma$) AND K^0. ROUGHLY EQUAL NUMBERS OF π^+, π^0 & π^- ARE PRODUCED.

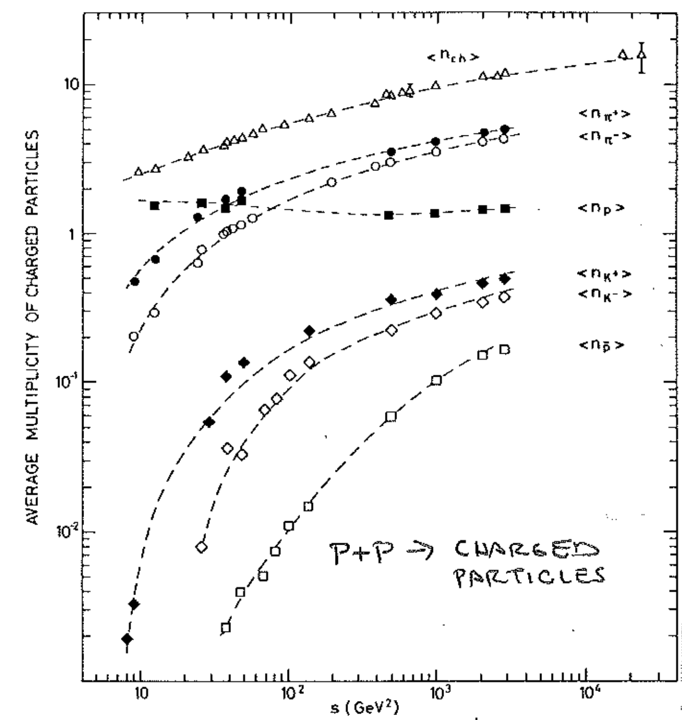

THE PARTICLE MULTIPLICITY DISTRIBUTION IS APPROXIMATELY A POISSON DISTRIBUTION, AS WOULD BE EXPECTED FROM STATISTICAL CONSIDERATIONS.

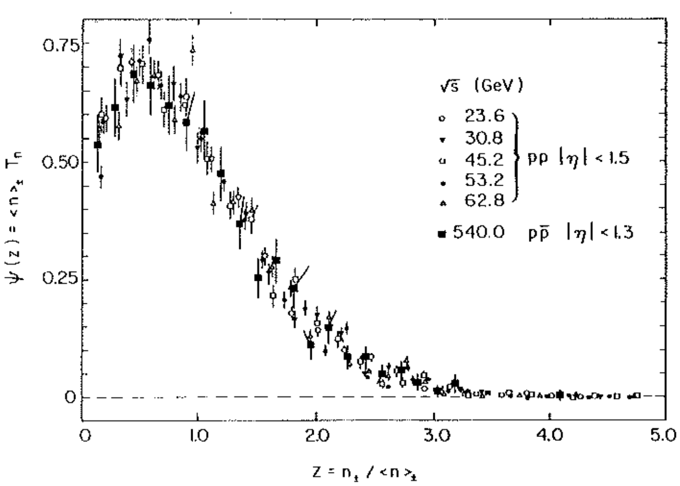

Fig. 3. The charged particle multiplicity $n_\pm$ in our fiducial region. T_n is the probability for the observation of n tracks and $\langle n \rangle_\pm = 6.57$ is the mean number per event.

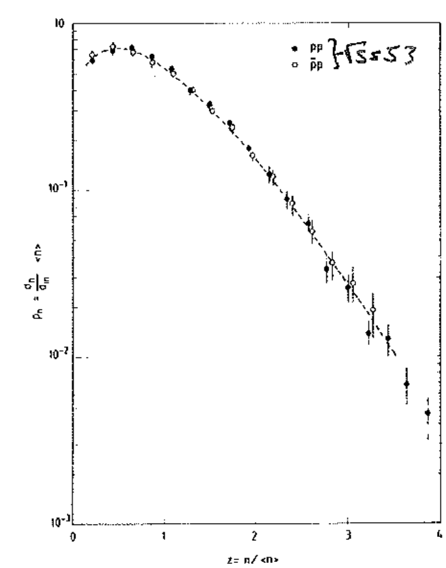

Fig. 4. The observed charged multiplicity distributions in pp and $\bar{p}p$ collisions for $|\eta| < 1.3$ expressed in the KNO scaling form. The dashed line is a fit to the experimental data at $\sqrt{s} = 540$ GeV.

EMPIRICALLY THE MULTIPLICITY DISTRIBUTION OBEYS A SCALING LAW, THAT $P(z)$ IS INDEPENDENT OF ENERGY, WHERE $z = n/\langle n \rangle$. THIS IS CALLED KNO SCALING (KOBA - NIELSEN - OLSSEN, I THINK)
A TRUE POISSON DISTRIBUTION OBEYS $P_n = \frac{\langle n \rangle^n e^{-\langle n \rangle}}{n!}$ WHICH DOES NOT EXHIBIT THIS SCALING BEHAVIOR.
THE SCALING FUNCTION $P(z)$ DOES DEPEND ON THE INITIAL STATE IN PRINCIPAL, BUT PP AND $\bar{p}p$ DISTRIBUTIONS APPEAR RATHER IDENTICAL.

ANOTHER STRIKING FEATURE OF MULTIPARTICLE PRODUCTION IS THAT THE AVERAGE TRANSVERSE MOMENTUM OF ALL TYPES OF PARTICLES IS

$$\langle p_t \rangle \sim 300 \text{ MeV/c}$$

IN THE FOLLOWING, 'LONGITUDINAL' AND 'TRANSVERSE' ARE REFERRED TO THE DIRECTIONS OF THE INITIAL STATE MOTION IN THE C.M. FRAME.
THE FACT THAT $\langle p_t \rangle \sim 300$ MeV/c HAS BEEN KNOWN SINCE THE '50'S FROM STUDIES OF COSMIC RAY SHOWERS. THE FIGURE SHOWS A RECENT CONFIRMATION OF THIS.

A SIMPLE PARAMETRIZATION OF THE CROSS SECTION FOR PRODUCTION OF A PARTICLE OF TRANSVERSE MOMENTUM p_t IS

$$\frac{d\sigma}{dp_t} \sim p_t e^{-bp_t} \Rightarrow \langle p_t \rangle = 2/b$$

EMPIRICALLY, $b \sim 6$ [GeV/c]$^{-1}$

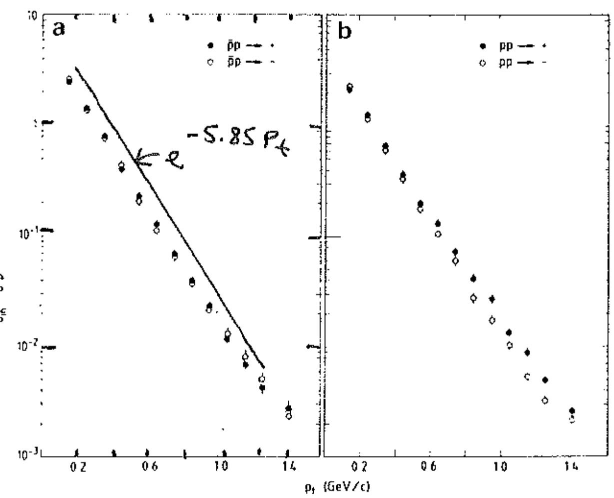

. p_t distributions for the production of positive and negative particles in (a) $\bar{p}p$ and (b) pp collisions at $\sqrt{s} = 53$ GeV.

IN THE LITERATURE (AS IN THE FIGURE ABOVE) ONE OFTEN FINDS A DIFFERENT FORM - THE SO-CALLED INVARIANT CROSS SECTION

$$E\frac{d\sigma}{d^3\bar{p}} = E\frac{d\sigma}{dp_{\parallel}\, dp_t^2}$$

OF COURSE, $d^3\bar{p}/E$ IS THE LORENTZ INVARIANT PHASE VOLUME SEEN EARLIER. ON SEPARATING $d^3\bar{p}$ INTO LONGITUDINAL AND TRANSVERSE FACTORS, WE FIND $dy = dp_{\parallel}/E$ AS AN INTERESTING QUANTITY.

INTEGRATING THIS WE DEFINE $y \equiv \frac{1}{2}\ln\left(\frac{E+p_{\parallel}}{E-p_{\parallel}}\right) =$ RAPIDITY

THIS UNLIKELY APPEARING QUANTITY IS QUITE USEFUL IN DISCUSSING MULTIPARTICLE PRODUCTION. A TECHNICAL ADVANTAGE IS ITS

EXCELLENT BEHAVIOR UNDER LORENTZ TRANSFORMATIONS ALONG THE DIRECTION OF MOTION OF THE INITIAL STATE (SUCH AS THE LAB TO C.M. FRAME BOOST). NAMELY, $L(y) = y' = y + \Delta$

WHERE Δ DOES NOT DEPEND ON y. IF TWO PARTICLES ARE SEPARATED BY A RAPIDITY GAP Δy IN ONE FRAME, THE SIZE OF THE GAP IS THE SAME IN ANY OTHER FRAME (WITH BOOST COLLINEAR TO INITIAL STATE MOTION).

THE EMPIRICAL INTEREST IN THE RAPIDITY VARIABLE IS THAT MULTIPARTICLE PRODUCTION APPEARS TO BE RATHER UNIFORM IN y, ESPECIALLY AT VERY HIGH ENERGIES.

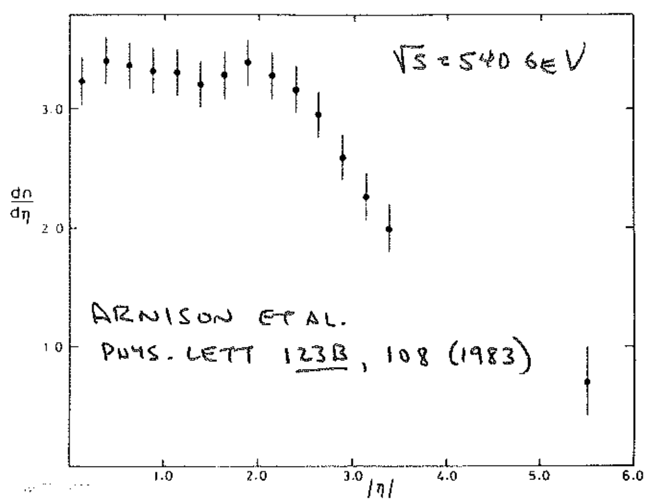

Fig. 1. Pseudo-rapidity density distributions for all charged multiplicities corrected for acceptance and backgrounds but excluding single diffraction events.

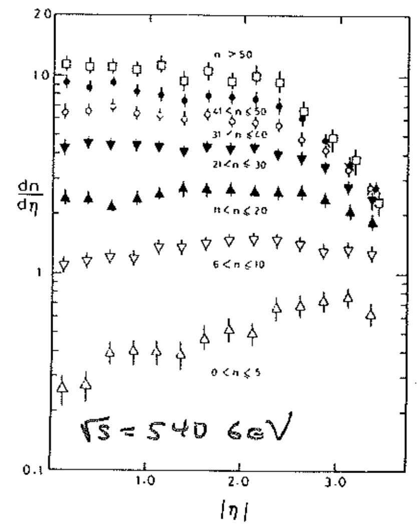

Fig. 2. Pseudo-rapidity density distributions for various intervals of observed charged multiplicity corrected for acceptance and backgrounds.

THUS $\dfrac{d\sigma}{dy} \sim$ CONSTANT. THEN $E\dfrac{d\sigma}{d^3p} = \dfrac{d\sigma}{dy\, dp_t^2} \sim \dfrac{d\sigma}{p_t\, dp_t} \sim e^{-6p_t}$

AT HIGH ENERGIES, $E_i \gg m_i$ HOLDS FOR EACH PARTICLE i PRODUCED, WHICH ALLOWS A CONVENIENT APPROXIMATION:

$$E = \sqrt{p^2 + m^2} \sim p = \frac{p_\parallel}{\cos\theta}$$

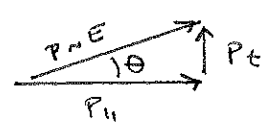

$$\text{So } y \sim \frac{1}{2}\ln\frac{1+\cos\theta}{1-\cos\theta} = -\ln\tan\theta/2$$

$$\eta \equiv -\ln\tan\theta/2 = \underline{\text{PSEUDO RAPIDITY}}$$

THE PSEUDORAPIDITY CAN BE MEASURED SIMPLY BY OBSERVING A PARTICLES DIRECTION, WITHOUT MEASURING ITS MOMENTUM, AND AS SUCH WAS A FAVORITE VARIABLE OF COSMIC RAY PHYSICISTS. SINCE $\langle p_t\rangle \sim 300$ MeV/c, WE CAN ALWAYS ESTIMATE $E \sim p \sim \dfrac{300\text{ MeV/c}}{\sin\theta}$ — A POOR MAN'S DATA ANALYSIS.

6. PARTON MODEL

EVEN THE BASIC FEATURES OF MULTIPARTICLE PRODUCTION SKETCHED ABOVE ARE NOT UNDERSTOOD IN ANY DETAIL IN TERMS OF OUR PRESENT THEORIES OF THE STRONG INTERACTION OF QUARKS AND GLUONS. THE MULTIPARTICLE INTERACTION IS JUST TOO COMPLICATED. IT REMAINS A CHALLENGE THAT WHILE OUR MODERN IDEAS CAN EXPLAIN MANY SUBTLE THINGS, THE MOST OBVIOUS FEATURES OF HIGH ENERGY PROCESSES REMAIN UNACCOUNTED FOR WITH ANY PRECISION.

APPROXIMATE UNDERSTANDING OF THESE FEATURES CAN BE GOTTEN FROM SIMPLE MODELS WHICH ARE INDEPENDENT OF THE EXACT DETAILS OF THE STRONG INTERACTION. THUS THE ROUGH CONSTANCY OF THE TOTAL CROSS SECTION VS. ENERGY IS CONSISTENT WITH A SHORT RANGE INTERACTION OF RANGE $R \sim 1$ FERMI. THE FULL INSIGHT OF QUANTUM CHROMODYNAMICS (QCD) HARDLY IMPROVES ON THIS. MANY OTHER FEATURES CAN BE UNDERSTOOD IN THE PARTON MODEL OF FEYNMAN, P. R. D2, 1267 (1970).

IN THIS MODEL MESONS AND BARYONS CONTAIN A NUMBER OF CONSTITUENTS CALLED PARTONS. IT IS NOT NECESSARY TO IDENTIFY THEM WITH QUARKS AND GLUONS (ALTHOUGH SUCH IDENTIFICATION IS EVENTUALLY ENCOURAGED). MULTIPARTICLE PRODUCTION ARISES OUT OF INTERACTIONS AMONG THE PARTONS.

A 'PREDICTION' ABOUT THE AVERAGE TRANSVERSE MOMENTUM FOLLOWS AT ONCE. THE PARENT PARTICLE CONFINES THE PARTONS WITHIN A RADIUS OF $\sim$ 1 FERMI. HENCE THE PARTONS MUST HAVE MOTION INSIDE THE PARENT OF MOMENTUM

$$P \sim \hbar/r \sim 200 \text{ MeV}/c \qquad \text{(FERMI MOTION)}$$

WHEN 2 PARTONS INTERACT TO FORM A FINAL STATE PARTICLE, THE LATTER WILL CARRY AWAY TYPICALLY $\sqrt{2}\cdot$ TRANSVERSE MOMENTUM OF EACH PARTON $\Rightarrow \langle P_t \rangle \sim 300$ MeV/c.

OTHER SIMPLE PREDICTIONS CONCERN THE LONGITUDINAL MOMENTUM DISTRIBUTION OF THE FINAL STATE PARTICLES. TWO CASES ARE DISTINGUISHED: WHEN THE FINAL STATE PARTICLE HAS A LARGE OR SMALL FRACTION OF THE MOMENTUM OF THE INITIAL STATE. A NATURAL VARIABLE IN THIS DISCUSSION IS THE FEYNMAN X

$$x_F \equiv \frac{P_\parallel}{P_{\parallel\,MAX}} \sim \frac{2P_\parallel}{\sqrt{s}} = \text{FRACTION OF POSSIBLE LONGITUDINAL MOMENTUM CARRIED BY THE FINAL STATE PARTICLE.}$$

WHEN x_F IS LARGE ($\gtrsim 0.1$) THE ENERGY OF THE FINAL STATE PARTICLE IS LARGE COMPARED TO ANY MASS SCALE OF THE INTERACTION (AT LEAST IF $\sqrt{s} > 10$ GeV). THEN WE MAY

EXPECT THAT THE OBSERVED DISTRIBUTION OF FINAL STATE PARTICLES IN x_F, $f(x_F)\,dx_F$ WILL NOT DEPEND ON $\sqrt{s}$, M, OR ANY OTHER ENERGY (EXCEPT POSSIBLE P_t). THIS IS THE IDEA OF FEYNMAN SCALING WHICH WAS VERIFIED AT THE PARTICLE ACCELERATORS BUILT DURING THE 1970'S.

A TYPICAL FORM OF THE SCALING DISTRIBUTION IS $f(x_F) \sim (1-x_F)^a$

WITH a SOME CONSTANT, WHICH FEYNMAN FEELS IS RELATED TO REGGE TRAJECTORIES.

THE FIGURE IS FROM CAREY ET AL, P.R.L. 33, 330 (1974). THEY FEEL THAT

$x_R = \frac{2P}{\sqrt{s}}$ IS AN EVEN BETTER SCALING VARIABLE THAN x_F

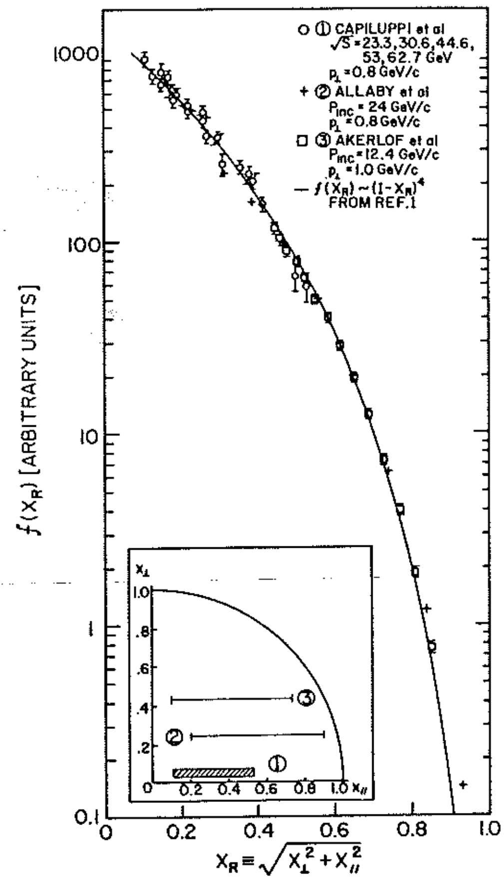

FIG. 1. Invariant cross sections for $p+p \to \pi^- +$ anything plotted versus x_R for fixed $p_\perp$. The solid curve represents the x_R dependence found in our experiment. Arbitrary normalization shifts have been made to illustrate the agreement in the x_R dependence. The inset shows the values of $x_\perp \equiv p_\perp/p_{max}{}^*$ and $x_\parallel \equiv p_\parallel{}^*/p_{max}{}^*$ covered by the three sets of data points.

IN THE SMALL x_F LIMIT THE SCALING IS NOT NECESSARILY EXPECTED TO HOLD, AS THEN THE PARTON ENERGIES APPROACH, SAY, 1 GeV, A TYPICAL MASS SCALE OF THE PARTICLES. THUS FOR $x_F \lesssim 1\,\mathrm{GeV}/\sqrt{s}$ WE NEED ANOTHER VIEW. FROM THE FIGURE ABOVE WE SEE THAT THE LOW x_F REGION IS WHERE MOST OF THE MULTIPARTICLE PRODUCTION TAKES PLACE. THIS IS UNDERSTOOD BY A PARTON MODEL ARGUMENT.

IF 2 PARTONS FROM THE INITIAL STATE PARTICLES COMBINE TO FORM A FINAL STATE PARTICLE, THE INTERACTION IS UNLIKELY IF THE PARTON MOMENTA MUST CHANGE A LOT

UNLIKELY

MORE PROBABLE

LOW x_F PARTICLE PRODUCTION IS 'CLEARLY' FAVORED.

THE DISTRIBUTION OF PARTONS AT SMALL X_F IS GOVERNED BY A PROCESS WHICH MUST BE SIMILAR TO BREMSSTRAHLUNG. THE INTERACTIONS AMONG LARGER X_F PARTONS CAUSE 'RADIATION' OF SMALL X_F PARTONS, PRODUCING A BREMSSTRAHLUNG-LIKE SPECTRUM dx_F/x_F. THE DIVERGENCE IN THIS EXPRESSION IS NEATLY AVOIDED IF WE NOTE $dx_F/x_F = dP_\parallel/P_\parallel \sim dP_\parallel/E = dy$; AND WE GET A RELATIVISTICALLY INVARIANT DESCRIPTION IN THE BARGAIN. THUS WE INFER THAT THE SMALL X_F PARTONS ARE UNIFORMLY DISTRIBUTED IN RAPIDITY. WHEN PARTONS COMBINE TO FORM FINAL STATE PARTICLES, THESE WILL BE UNIFORMLY DISTRIBUTED IN RAPIDITY ALSO. AS WE SAW ON p 224 THIS SEEMS TO BE THE CASE EXPERIMENTALLY!

BY RECALLING THAT $\langle P_t \rangle \sim .3$ GeV/c WE ESTIMATE THAT THE MAXIMUM RAPIDITY IS $y_{MAX} \sim \frac{1}{2} \ln \frac{s}{.05}$ (IN C.M. FRAME)

WE THEN EXPECT THAT THE TOTAL NUMBER OF PARTICLES PRODUCED WILL VARY AS $y_{MAX} \sim \ln s$, AS SEEN ON p 222.

FEYNMAN GIVES ANOTHER ARGUMENT TO SUPPORT THE LAST CONCLUSION. THE MULTIPARTICLE PRODUCTION PROCESS IS STATISTICAL IN NATURE, SO THE MULTIPLICITY DISTRIBUTION WILL BE POISSON-LIKE. ACTUALLY

$$P(n) \sim \frac{\langle n\rangle^{n-2} e^{-\langle n\rangle}}{(n-2)!}$$

SINCE EVEN THE SIMPLEST FINAL STATE HAS 2 PARTICLES, IT IS THE QUANTITY $n-2$ WHICH FLUCTUATES. IN THIS CASE THE PROBABILITY OF HAVING A 2 BODY FINAL STATE IS $\sim e^{-\langle n\rangle}$. BUT FROM OUR REGGE MODEL (p 220) $\sigma_{2BODY} \sim s^{2a-1}$

WITH a = INTERCEPT OF SOME RELEVANT REGGE TRAJECTORY. NOTING THAT $\sigma_{TOTAL} \sim$ CONSTANT, WE HAVE

$$P(2) \sim s^{2a-1} = e^{-\langle n\rangle} \Rightarrow \langle n\rangle \sim 1 - 2a \ln s$$

WE HOPE THAT IN THE FUTURE THESE PARTON MODEL ESTIMATES WILL BE REPLACED BY MORE SUBSTANTIAL CALCULATIONS, PERHAPS BASED ON THE QCD THEORY OF QUARKS AND GLUONS.

7. LARGE TRANSVERSE MOMENTUM PHENOMENA

AN ASPECT OF THE STRONG INTERACTION AT HIGH ENERGIES HAS EMERGED THAT MAY ALLOW A MORE FUNDAMENTAL ANALYSIS. THIS IS THE OBSERVATION OF PARTICLE PRODUCTION AT VERY LARGE TRANSVERSE MOMENTUM.

THE FIRST INDICATION OF THIS PHENOMENON CAME IN 1972, WHEN A STRIKING EXCESS OF π^0 MESONS WAS OBSERVED AT HIGH TRANSVERSE MOMENTUM AT 90° TO THE BEAM DIRECTION IN pp COLLISIONS. AS SEEN IN THE FIGURE, THE PRODUCTION CROSS SECTION IS MUCH FLATTER THAN e^{-6p_t} WHICH WOULD BE EXTRAPOLATED FROM THE LOW p_t REGIME DISCUSSED ON p. 223.

Fig. 16.2. Invariant cross-section for $pp \to \pi^0 X$ at large p_T compared with the extrapolation (solid curve) of the exponential behaviour at lower p_T. (Data from CERN-Columbia-Rockefeller-Saclay collaboration.)

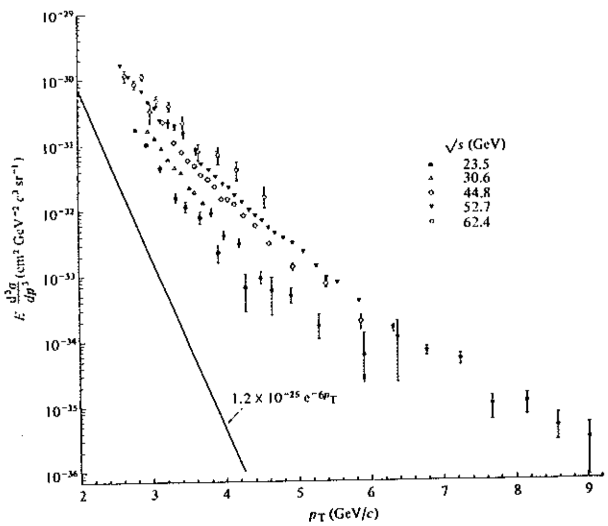

Fig. 16.3. Large p_T data for $pp \to \pi^0 X$ plotted so as to check the scaling form (16.2.4). (Data from CERN–Columbia–Rockefeller–Saclay collaboration.)

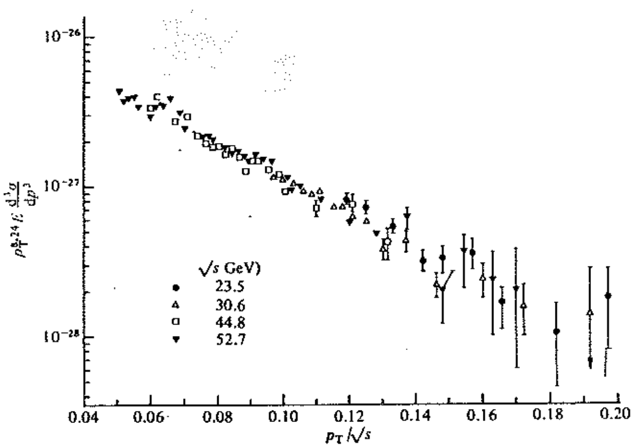

DATA COLLECTED AT SEVERAL ENERGIES WERE FOUND TO OBEY A POWER LAW BEHAVIOR $E\, d\sigma/d^3p \sim 1/p_t^{\,8}$.

THE SPECULATION IS THAT THE HIGH p_t π^0'S ARE DUE TO RARE, HARD SCATTERING BETWEEN TWO QUARKS. THIS IS QUITE DIFFERENT FROM OUR PICTURE OF LOW p_t PARTICLE PRODUCTION DOMINATED BY LOW x_F PARTON INTERACTIONS. THE SCATTERED QUARK IS NOT DETECTABLE IN THE LABORATORY DUE TO QUARK CONFINEMENT; INSTEAD IT 'DRESSES' ITSELF WITH OTHER PARTONS BEFORE LEAVING THE pp INTERACTION. IN THE LABORATORY ONE MIGHT SEE A SERIES OF MESONS ALIGNED ALONG THE QUARK DIRECTION, FORMING A 'JET' OF PARTICLES. IF THE HIGHEST ENERGY 'FRAGMENT' OF THE QUARK IS A π^0 MESON, THIS COULD LEAD TO THE OBSERVED HIGH p_t π^0 PRODUCTION.

EXPERIMENTS SOON FOLLOWED THE INITIAL RESULT TO LOOK FOR THE ENTIRE 'JET'. BUT EVEN WITH 10 GEV ENERGY IN A 'JET' THE LABORATORY DISTRIBUTION OF THE RELATED PARTICLES IS RATHER BROAD, AND THE EARLY JET STUDIES WERE NOT COMPLETELY CONVINCING. ANOTHER DIFFICULTY WITH THE QUARK-QUARK SCATTERING PICTURE IS THE $1/p_t^8$ DEPENDENCE. IF THE

QUARK-QUARK SCATTERING WERE REALLY DUE TO THE EXCHANGE OF MASSLESS GLUONS, THEN THE CROSS SECTION SHOULD VARY LIKE $1/p_t^4$ - JUST AS IN RUTHERFORD SCATTERING VIA 1 PHOTON EXCHANGE (RECALL $d\sigma/dq^2 \sim 1/q^4$ AND $q \leftrightarrow p_t$ WHEN $\theta = 90°$)

PLAUSIBLE EVIDENCE FOR QUARK JETS WAS FOUND IN THE LATE 1970'S IN THE REACTION $e^+e^- \to q\bar{q} \to 2$ JETS. THIS ALLOWED

MEASUREMENT OF THE PROCESS QUARK $\to$ JET, AND HAS LED TO MANY QCD CALCULATIONS, SUCH AS THAT IN THE FIGURE BELOW FIELD, PHYS. LETT B135, 204 (1984)

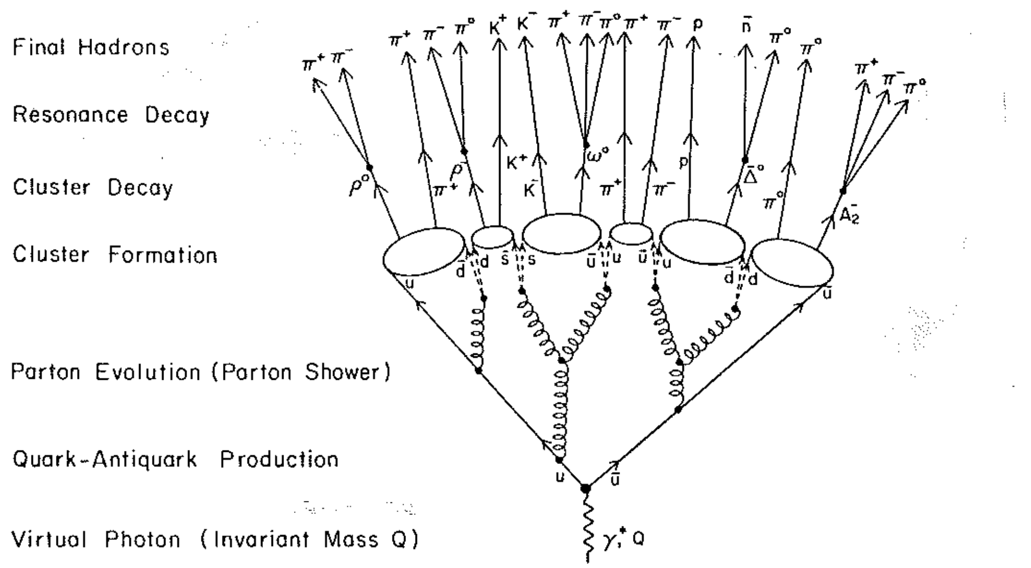

Fig. 1. Illustration of the QCD parton-shower phase-space approach. The initial quark and antiquark produced by the "decay" of a virtual photon of invariant mass, Q, are allowed to bremsstrahlung gluons until their invariant masses have been degraded to some cut-off mass, μ_C. The invariant masses of the radiated partons are kinematically constrained to be less than those of their parents with the difference being converted into the transverse momentum of the emitted partons. The radiated partons themselves radiate more partons, producing a "parton shower". Color singlet subsystems or "clusters" are formed by forcibly splitting each final state gluon into a quark–antiquark pair. These clusters are then allowed to "decay" isotropically via two-body phase-space. The model does not rely on the Field–Feynman jet parameterization, but instead follows more closely perturbative QCD.

WITH THE LARGE CENTER OF MASS ENERGY ($\sqrt{s} = 540$ GEV) AVAILABLE AT THE CERN $\bar{p}p$ COLLIDER, THE JET STUDIES HAVE BECOME MUCH MORE CLEARCUT. JETS WITH ~ 50 GEV ENERGY ARE ILLUSTRATED ON THE NEXT PAGE [ARNISON ET AL PHYS LETT 123B, 115 (1983)].

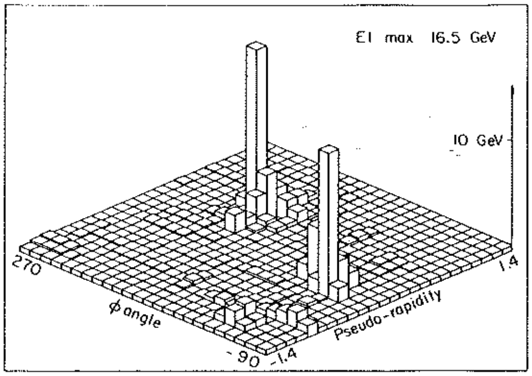

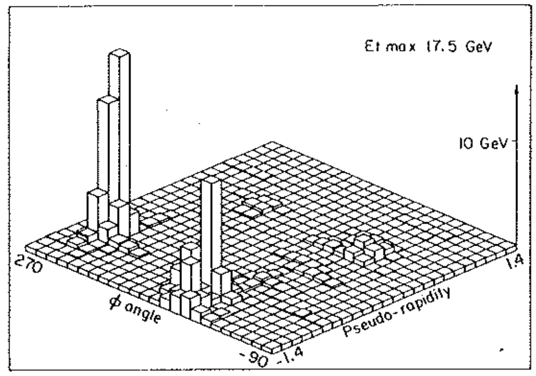

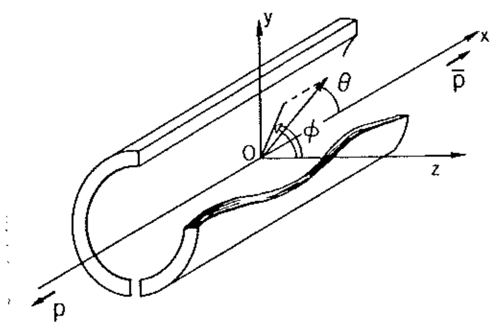

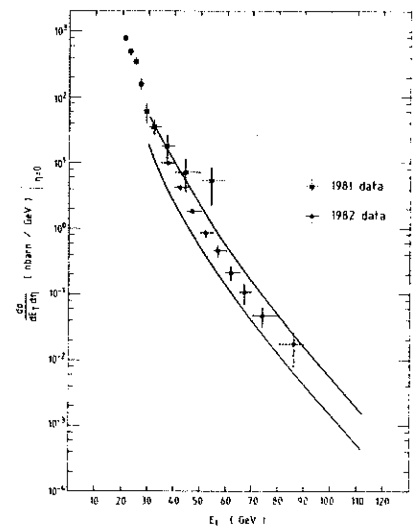

Fig. 3. Inclusive jet cross section $d\sigma/dE_T d\eta$ ($\eta = 0$) as function of E_T. 1981 data (X) and 1982 data (+). The hatched band corresponds to possible QCD predictions [14].

AS THE ENERGY RATHER THAN MOMENTUM OF THE JET PARTICLES IS MEASURED IN A HADRON CALORIMETER, RESULTS ARE PRESENTED IN TERMS OF E_t RATHER THAN P_t. THE VERY HIGH E_t CROSS SECTION VARIES LIKE $1/E_t^{4 \text{ or } 5}$ MUCH MORE CONSISTENT WITH THE QUARK-QUARK SCATTERING IDEA.

THE FIGURES BELOW SHOW DISTRIBUTIONS OF PARTICLES WITHIN A JET. [P.L. 132B, 220 (1983)]

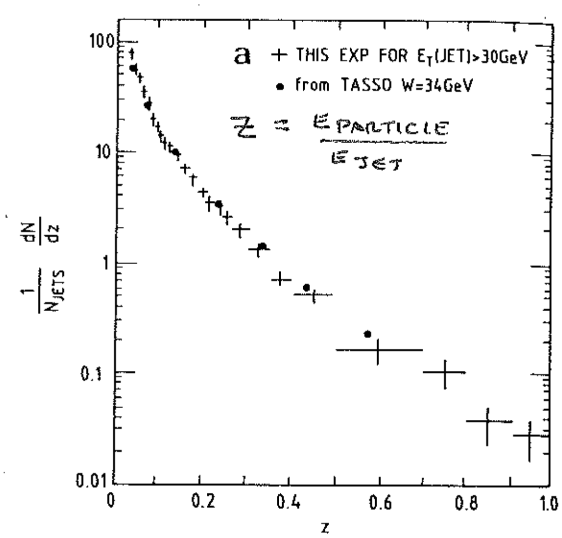

Fig. 2. (a) Charged-particle fragmentation function for E_T(jet) > 30 GeV, compared with similar results from the TASSO detector at PETRA at W = 34 GeV.

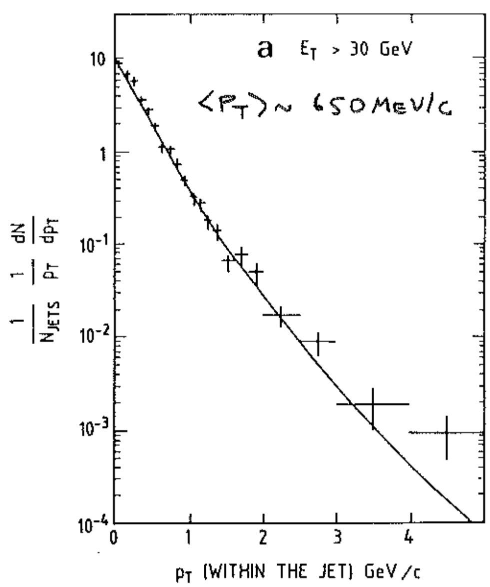

Fig. 4 (a) $(1/p_T)(dN/dp_T)$ spectrum (p_T with respect to the jet axis) for charged particles with $z > 0.1$. The solid line is the result of a fit $1/(p_T + p_{T_0})^N$ with p_{T_0} = 4.0 GeV/c, N = 14.8.